

A Study on Micro-Machining Technology for the Machining of NiTi: Five-Axis Micro-Milling and Micro Deep-Hole Drilling

D. Biermann, F. Kahleyss, E. Krebs, and T. Upmeier

(Submitted May 6, 2010; in revised form September 17, 2010)

Micro-sized applications are gaining more and more relevance for NiTi-based shape memory alloys (SMA). Different types of micro-machining offer unique possibilities for the manufacturing of NiTi components. The advantage of machining is the low thermal influence on the workpiece. This is important, because the phase transformation temperatures of NiTi SMAs can be changed and the components may need extensive post manufacturing. The article offers a simulation-based approach to optimize five-axis micro-milling processes with respect to the special material properties of NiTi SMA. Especially, the influence of the various tool inclination angles is considered for introducing an intelligent tool inclination optimization algorithm. Furthermore, aspects of micro deep-hole drilling of SMAs are discussed. Tools with diameters as small as 0.5 mm are used. The possible length-to-diameter ratio reaches up to 50. This process offers new possibilities in the manufacturing of microstents. The study concentrates on the influence of the cutting speed, the feed and the tool design on the tool wear and the quality of the drilled holes.

Keywords machining, micro deep-hole drilling, micro-milling, NiTi, shape memory alloys

1. Introduction

The potential of functional materials like NiTi SMA is of great interest in various fields of scientific research. This material offers many different application possibilities, especially in medical technologies, owing to its versatile properties like biocompatibility, superelasticity, and shape memory. Applications like medical implants that rely on these properties, call for reliable manufacturing technologies to create and machine various free-form surfaces or deep holes. For this purpose, five-axis micro-milling offers unique possibilities, especially, high material removal rates combined with good surface quality and very little thermal damage of the peripheral zone. In contrast to the conventional end milling cutters, the ball end mills can also machine at an inclination, hence allowing optimal process parameters instantaneously during machining. Furthermore, the ball nose cutters offer the possibility of five-axis machining processes that can realize the machining of complex workpiece geometries. Five-axis milling leads to varying loads on the tool that might result in early tool failure and also poor surface finish due to a

This article is an invited paper selected from presentations at Shape Memory and Superelastic Technologies 2010, held May 16-20, 2010, in Pacific Grove, California, and has been expanded from the original presentation.

D. Biermann, F. Kahleyss, E. Krebs, and T. Upmeier, Institute of Machining Technology, Technische Universitaet Dortmund, Dortmund, Germany. Contact e-mails: Biermann@isf.de and kahleyss@isf.de.

continuously changing contact zone. In addition to these challenges, NiTi is characterized by unsuitable chip formation. In principle, micro-milling (Ref 1), five-axis milling (Ref 2-7), and machining of NiTi SMA (Ref 8-10) have already been amply researched and, thus, are established in daily industrial practice. This work focuses on the development of a simulation-based optimization for numerical control (NC) programs which are based on the results of the fundamental experiments concerning the tool inclination angles in micro-milling of NiTi SMA using ball end mills (Ref 11, 12). The newly developed algorithm is not only capable of detecting unfavorable tool inclinations in the machining of free-form surfaces, but can also readjust them. The verification of the algorithm is accomplished by the machining of a reference workpiece. The second part of this article shows the first results concerning the micro deep-hole drilling of NiTi SMA obtained from experiments with tools having diameters as small as 1.5, 1, and 0.5 mm. The micro deep-hole drilling is challenging with regard to the tools as well as the process strategy. This results in very different characteristics of the processes if compared to that of the conventional deep hole drilling. Challenges include the drastically reduced stiffness of the tools and the chip evacuation out of the hole. The special properties of NiTi SMA add to the task of developing a reliable micro deep-hole drilling process strategy for these smart materials.

2. Experimental

2.1 Simulation of Milling Processes

The optimization algorithm to adapt the tool inclination angles is based on the simulation tool NCChip (Ref 13). There is a multitude of factors influencing the results of five-axis milling processes due to the complex tool engagement

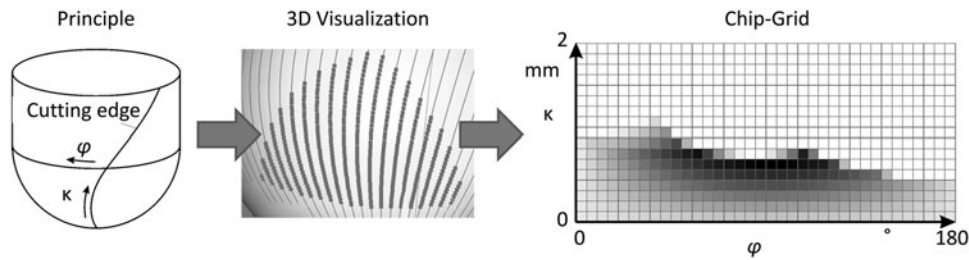


Fig. 1 Scheme for mapping the cutting edge points into a chip-grid (l) and chip-grid with the chip thickness (r) illustrated by a gray scale (Ref 13)

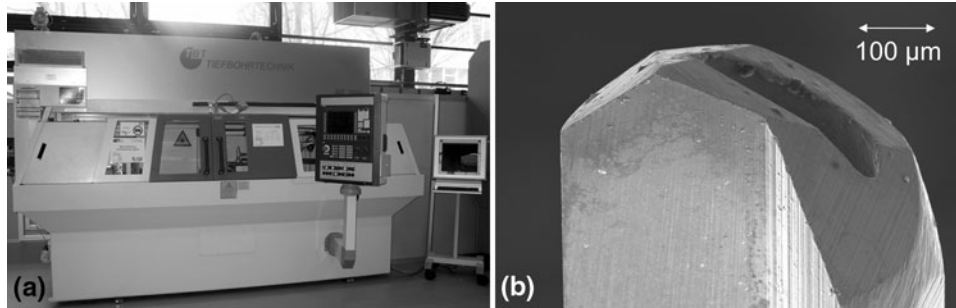


Fig. 2 (a) Machining center and (b) micro-single-lip drill with a diameter of $d = 0.5$ mm

situations. Different inclination angles cause a varying time-discrete chip cross section, thus creating varying chip thickness gradients, cutting force gradients and a cutting speed profile. To build up process models which can visualize and optimize the machining of free-formed surfaces it is necessary to use a geometric simulation that can produce accurate results even using complex tool paths. This modeling is based on the NC-programs generated by standard CAM-systems. For an accurate analytical calculation of the process forces, it is also necessary to take the rotation of the tool into account and to have a look at the phenomena occurring at the cutting edge. Therefore, the chip is converted into a chip-grid (Fig. 1) (Ref 13).

The chip-grid is a two-dimensional array which carries the process data for the corresponding points on the cutter hull. The two directions of the grid are the angle φ and the bow-length of the cutting edge l . So each grid unit $E(\varphi, l)$ carries the process information at an angle φ and a distance l along the cutting edge measured from the tip of the tool. Here, the gray scale represents the chip thickness r , whereas black chip-grid-entries represent the maximum chip thickness. This chip-grid carries all information which is required to optimize the tool inclination angles.

2.2 Micro-Milling and Micro Deep-Hole Drilling

Ball end mills made of cemented carbide with a diameter of $d = 1.0$ mm were used for verifying the milling optimization algorithm. These tools were coated with a thin TiAlN-layer. The milling experiments were conducted on a five-axis CNC machining center “DMU 50 eVolution” with a maximum spindle speed of 18,000 rpm. The measured accuracy of the machine tool is $\pm 2 \mu\text{m}$.

The micro deep-hole machining center used was a TBT ML-200. It is especially designed to apply single-lip drilling

tools having diameters of $d = 0.5, \dots, 6.0$ mm with a maximum available drilling depth of $l_t = 450$ mm. Its spindle speed reaches up to 36,000 rpm. The coolant can be applied with a maximum pressure of $p = 220$ bar. The machine features two separate working chambers. One of them contains a laser-drill unit with a pulse power of up to $p_p = 8$ kW. The workpiece can be transferred between the two chambers automatically to achieve a high accuracy. The tools that were used in the experiments are single-lip drills having diameters of 1.5, 1.0, and 0.5 mm. Various tool point angles as well as different coatings (uncoated, TiN-, and TiAlN-coating) were tested. Twist drills with a diameter of 1.0 mm were analyzed as well. Figure 2 shows the machine tool and a single-lip drilling tool with a diameter of 1.0 mm.

2.3 Machined Material

In this study, binary pseudoplastic NiTi bars (rolled, $\text{Ø}34.1$ mm) with a Ni-content of 50.2 at.% (oxide free surface) were examined. Its condition in the machining experiments was as received without further heat treatment. Differential scanning calorimetry (DSC) was performed, using a DSC Netzsch type CC 204 F1 to determine the phase transformation temperatures (Fig. 3). The material exhibits a one-step martensitic transformation upon cooling and a one-step reverse transformation back to austenite upon heating, its M_p temperature lies at 19,45 °C.

3. Results and Discussions

3.1 Analysis of the Milling Processes with the Chip-Grid Method

The simulation software NCChip can be utilized for manifold purposes. The applicability of the aforementioned

chip-grid method has been proven in a first step analyzing the geometric engagement conditions of the cutting edges of the ball end milling tools. Figure 4 depicts the three-dimensional chip thickness in the chip-grid for varied inclination angles β_f (tool inclination along the feed direction) and β_{fN} (tool inclination across the feed direction).

A median chip thickness gradient can be identified that proceeds from the center of the line with a chip thickness of zero to the point with the maximum chip thickness. This characteristic chip thickness gradient is orthogonal to the cutting direction at a high tool inclination of $\beta_f = 50^\circ$. These cutting conditions have been identified as the optimum in earlier experiments, whereas inclinations of $\beta_{fN} = 50^\circ$ generate a high tool wear and a poor surface quality (Ref 11, 12). The cutting direction parallels the median chip thickness gradient in the latter case. If the chip form in the chip-grid is reduced to the

area of the one-time contact between the tool and the workpiece, the resulting surface chip is a characteristic line in the chip-grid with a certain slope (Fig. 5). Since this surface chip is orthogonal to the median chip thickness gradient, it offers the same analytical options. At the same time, its numerical quantifiability is much easier to accomplish: At optimal cutting conditions the slope is zero, suboptimal cutting kinematics manifest in very high slopes.

This enables the definition of the objectives of the optimization algorithm. Small inclination angles β_f should be increased to avoid center cut conditions. The algorithm can detect too small inclination angles by defining a minimum limit for the κ -values in the chip-grid (Fig. 6). The adaptation of the tool inclination is implemented by the definition of a rotary axis in the simulation. Higher tool inclinations of β_{fN} can be detected by checking the slope of the surface chip form. The tool inclination can be adapted by rotating the tool around the surface normal. This causes a reduction in the slope of the surface chip (Fig. 6). Since the chip-grid method always considers the relative engagement situation of the tool with respect to the workpiece, it can be applied on any free-form surfaces and NC-programs.

3.2 Experimental Verification of the Simulation Algorithm

The described optimization algorithm is used to analyze and to optimize a CAM-generated, three-axis NC-program of an experimental workpiece made of NiTi SMA. Figure 7 depicts the process results for a workpiece machined using a three-axis strategy compared to the workpiece machined with the optimized NC-program. This optimized program is then a five-axis NC-program. The typical layerwise milling strategy of the three-axis NC-program is expected to produce a poor surface finish due to the ever increasing tool inclinations of β_{fN} that result from this strategy.

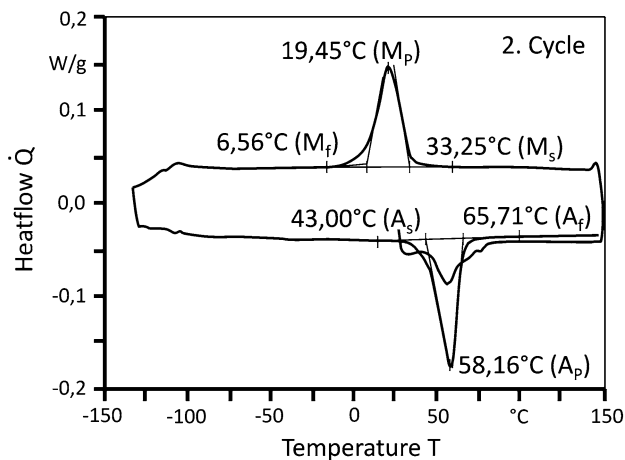


Fig. 3 DSC-analysis of the machined NiTi samples

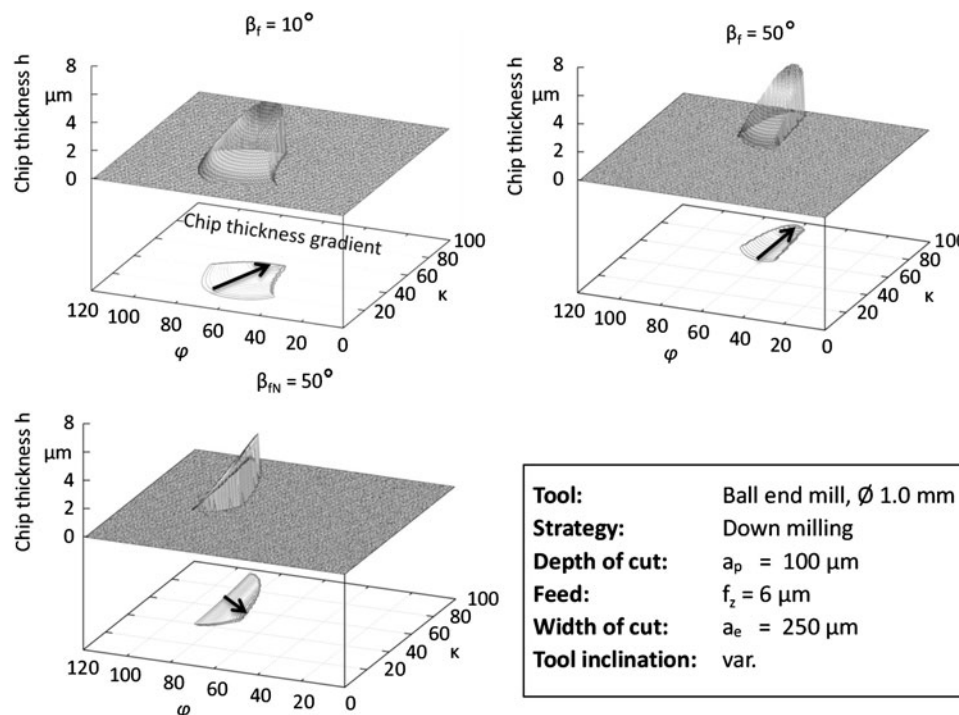


Fig. 4 Illustration of different chip-grid conditions for varied tool inclination angles

Tool:	Ball end mill \varnothing 1,0 mm
Strategy:	Down milling
Depth of cut:	$a_p = 100 \mu\text{m}$
Feed:	$f_z = 6 \mu\text{m}$
Width of cut:	$a_e = 250 \mu\text{m}$
Tool inclination:	var.

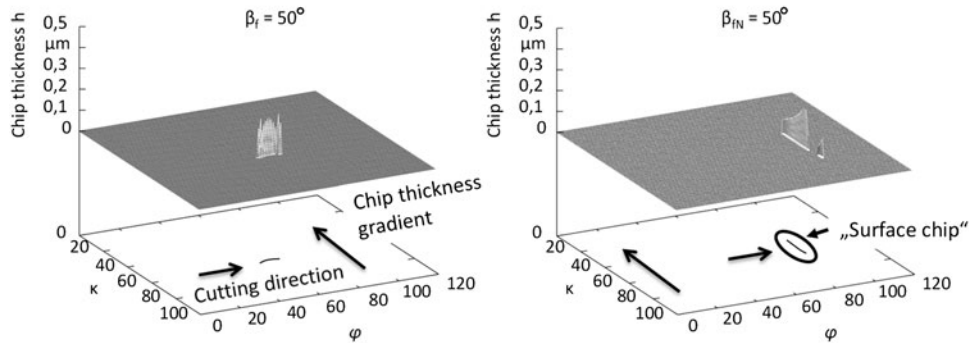
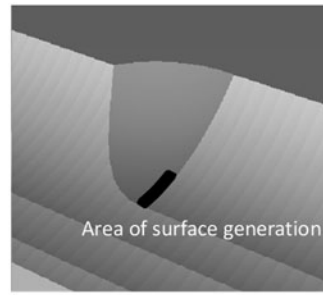


Fig. 5 Display of the surface chip in the chip-grid for optimal and suboptimal cutting conditions

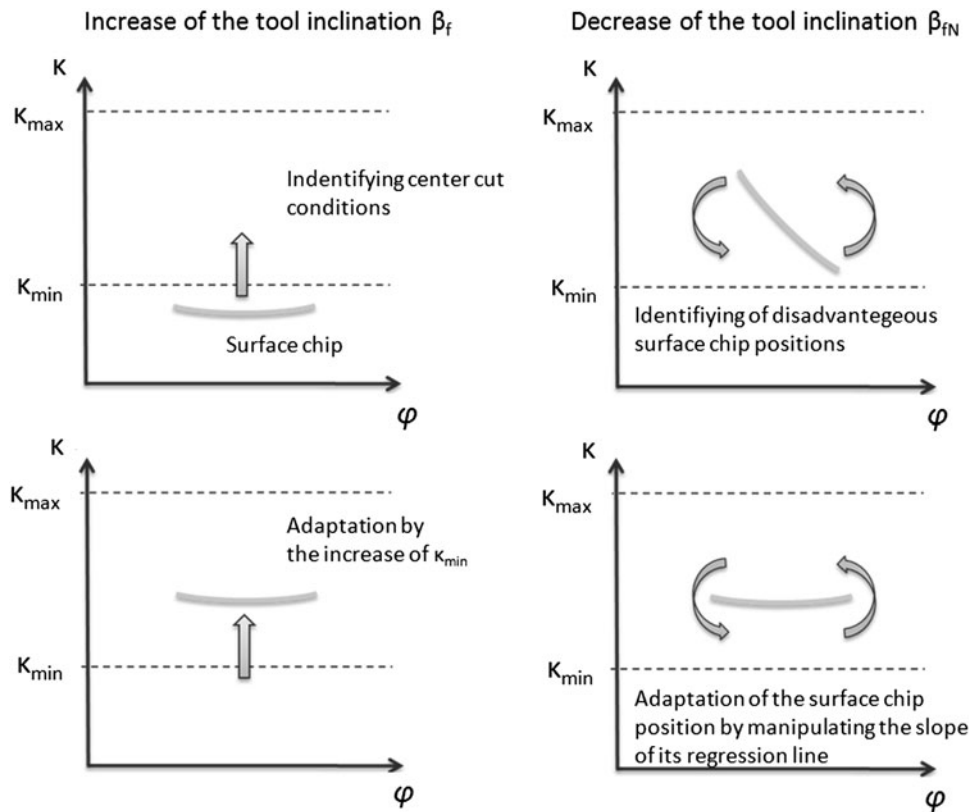


Fig. 6 Objective definition of the optimization algorithm in terms of surface chip conditions

The strongly differing quality of the workpiece surface is quite obvious. As expected, the three-axis workpiece has a very rough surface profile with a lot of adhesions of the workpiece material; whereas the five-axis workpiece features a very

evenly structured surface that equals the theoretical profile. This proves the effectiveness of the optimization algorithm to control the tool inclination in relation to the surface at any time during the machining of the workpiece.

Tool:	Ball end mill, ϕ 1.0 mm	Strategy:	Down milling	
Coating:	TiAlN (CC)	Workpiece:	NiTi	
Cutting sp.:	$v_{c,max} = 47$ m/min	Machined volume:	$V_z = 55$ mm ³	
Depth of cut:	$a_p = 100$ μ m	Feed:	$f_z = 6$ μ m	
Lubricant:	Emulsion	Width of cut:	$a_e = 250$ μ m	
Tool inclin.:	var.			

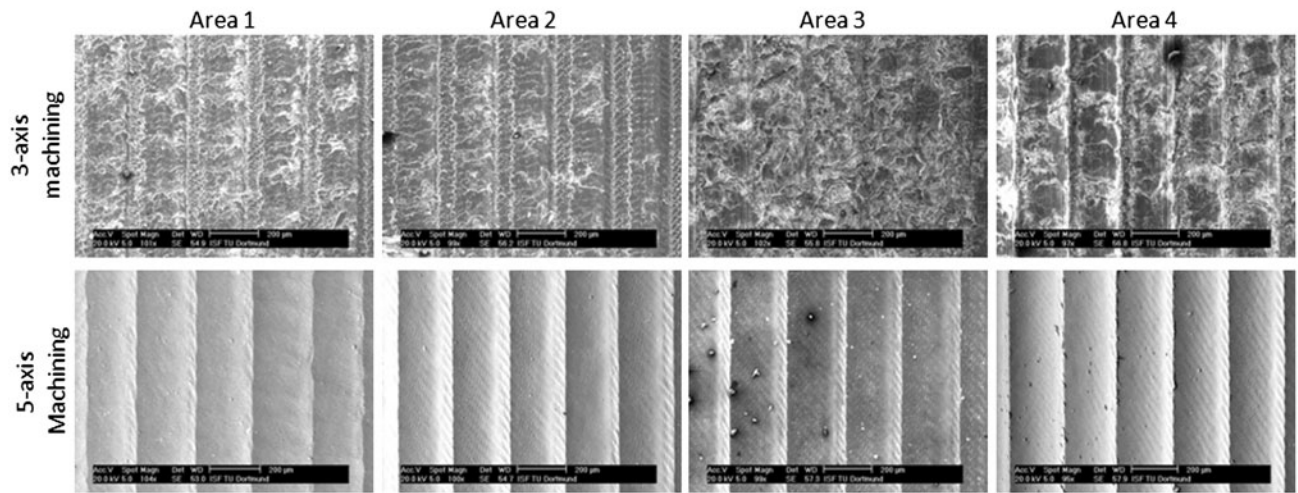


Fig. 7 Comparison of the process results: Three-axis versus five-axis machining

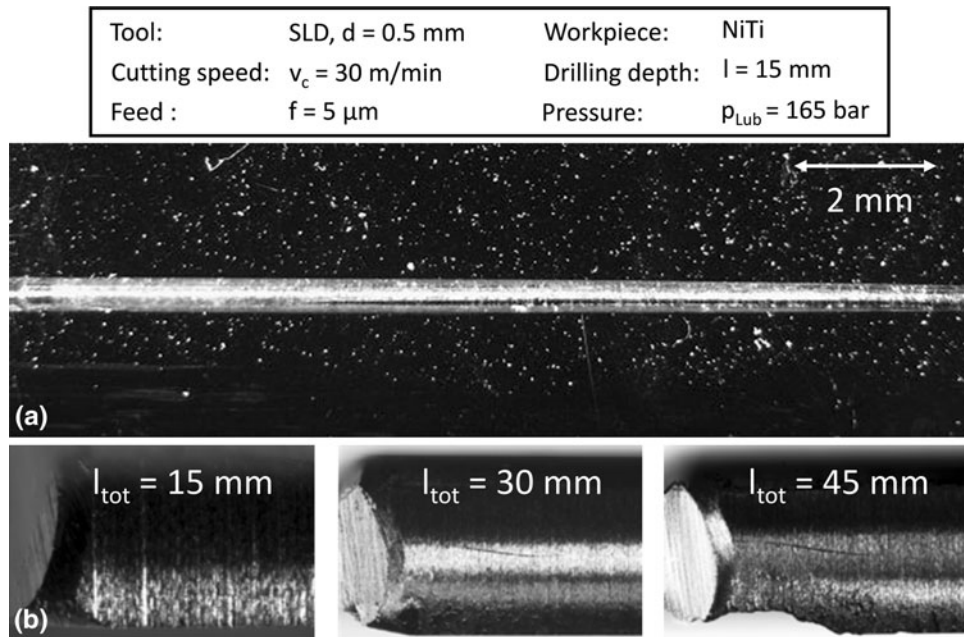


Fig. 8 (a) Drilled hole with a length of 15 mm ($d = 0.5$ mm) and (b) spontaneous adhesion wear at the guide pad

3.3 Micro Deep-Hole Drilling of NiTi SMA

The applicable cutting data for the micro deep-hole drilling of NiTi is very limited. Overall, the quality of the drilled holes is very good (Fig. 8a). Nevertheless, the single-lip drills suffer from adhesion on the guide pads. This can occur spontaneously after various drilling depths, or gradually over the total drilling depth (Fig. 8b).

This unpredictable behavior of the tools is due to the nature of their design and the properties of the NiTi SMA. The tools have an asymmetrical design of the cutting edge. This causes a radial force component that is absorbed by the so called guide pad. During drilling NiTi SMA, the friction between the guide pad and the wall of the hole leads to an increasing adhesion. This results in a continuous

Tool:	SLD, $d = 0.5 \text{ mm}$	Workpiece:	NiTi
Cutting speed:	$v_c = 30 \text{ m/min}$	Drilling depth:	$l = 15 \text{ mm}$
Feed :	$f = 5 \mu\text{m}$	Pressure:	$p_{\text{Lub}} = 165 \text{ bar}$

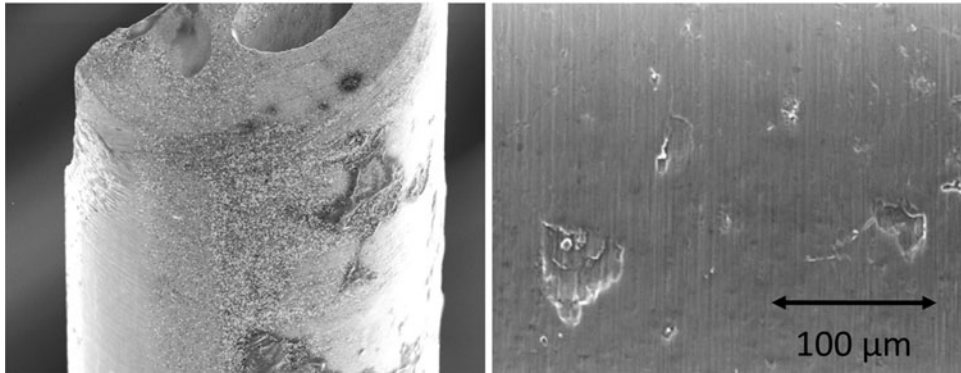


Fig. 9 Adhesion of NiTi on the guide pad and the hole wall

Tool:	TD, $d = 1.0 \text{ mm}$	Workpiece:	NiTi
Cutting speed:	$v_c = 30 \text{ m/min}$	Drilling depth:	$l = 20 \text{ mm}$
Feed :	var.	Pressure:	$p_{\text{Lub}} = 200 \text{ bar}$

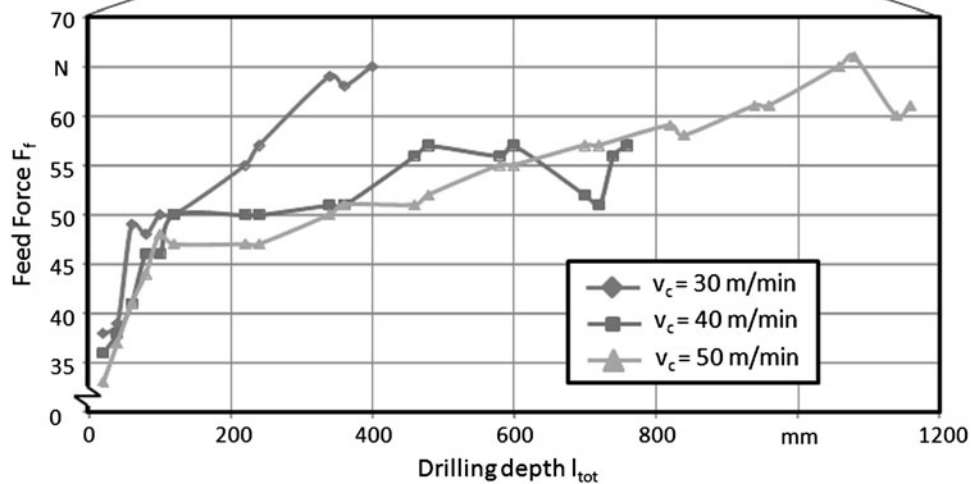
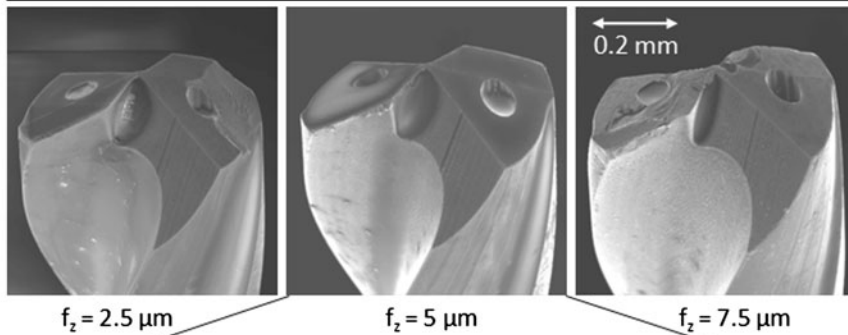


Fig. 10 Tool life and feed force of the twist drills against the cutting speed

microwelding process of the guide pad and the workpiece. Its effects are shown in Fig. 9.

Different strategies can be applied to minimize this effect. The use of single-lip drills with a smaller tip angle helps to

reduce the radial force component, thus reducing the adhesion on the guide pad. Furthermore, a coating of TiN or TiAlN also helps in decreasing the friction on the guide pads. The right choice of the cutting speed is mandatory for the most efficient

use of the drilling tools as well. The speed should not exceed $v_c = 30$ m/min. A lower cutting speed causes the chipping of the cutting edge due to high work-hardening. Higher speeds enhance the adhesion processes again. The optimum feed for tools with a diameter of $d = 1.0$ mm is $f = 5$ μm . If the tool diameter is reduced to 0.5 mm, the feed has to be adapted to only 0.5 μm to avoid tool breakage. This is true for all kinds of drilling tool concepts. However, the twist drills do not show adhesive wear at all. This is due to their symmetric design without a radial force component and their TiAlN coating. Without showing the main wear effects of the single-lip drills, the twist drills with a diameter of $d = 1.0$ mm reached a total drilling depth of up to 1200 mm; whereas the single-lip drilling tools achieved a maximum total drilling depth of only 420 mm. Figure 10 depicts the influence of the cutting speed on the achievable total drilling depth with regard to the varied cutting speeds.

The effect of the cutting speed concerning the tool life is contrary compared to the single-lip drills. The highest total drilling depth is achieved at a cutting speed of $v_c = 50$ m/min. Lower speeds lead to an earlier tool failure. Since the main wear mechanism (adhesion) is not too much pronounced, the cutting speed can be increased to reduce the work-hardening effects of the drilling process, thus reducing the overall process forces. Nevertheless, the feed force rises during the course of the experiments due to an increasing rounding of the cutting edge.

4. Conclusions

This article summarizes different aspects of the micro-machining of NiTi SMA. A simulation algorithm is presented that optimizes tool inclinations in the three- or five-axis micro milling processes. It is based on the geometric analysis of the various engagement conditions of the cutting edge. The definition of a surface chip allows the numerical correlation of the tool inclination in relation to the workpiece surface and the quality of the machined workpiece, thus allowing the programming of the optimization algorithm. Its effectiveness has been proven by the machining of a reference workpiece. The investigations of the micro deep-hole drilling showed promising results. Holes having diameters as small as 0.5 mm and a depth of up to 15 mm can be machined with a high quality. The adhesion wear of the single-lip drills at the guide pad reduces their tool life considerably. Twist drills reach a much higher total drilling depth at much higher cutting speeds, thus representing the most effective way to drill NiTi SMA. The reason for their superior machining characteristics is the

presence of a symmetric load due to process forces without radial components. This reduces the friction between the tool and the hole wall. The minimization of adhesion wear allows the higher cutting speeds which reduces the cutting forces due to a decreased work-hardening.

Acknowledgments

The authors acknowledge funding from the German Research Foundation (DFG) and NRW through the Special Research Center SFB 459 (Shape Memory Technology).

References

1. B. Damazo, A Summary of Micro-Milling Studies, *Proc. of the EuSPEN*, Bremen, Germany, May, p 322-325, 1999
2. J.H. Camacho, "Frästechnologie für Funktionsflächen im Formenbau," Dissertation, Universität Hannover, 1991
3. S. Hock, "Hochgeschwindigkeitsfräsen im Werkzeug- und Großformenbau-Eingriffsverhältnisse und Technologie," Dissertation, TU Darmstadt, 1996
4. D. Janovsky, "Einfluss der Technologie auf Maßgenauigkeit und Prozesssicherheit beim Hochgeschwindigkeitsfräsen im Werkzeug- und Formenbau," Dissertation, TU Darmstadt, 1996
5. Y. Wang and X. Tang, Five-Axis NC Machining of Sculptured Surfaces, *Int. J. Adv. Manufact. Technol.*, 1999, **15**, p 7-14
6. F. Klocke, M. Reuber, and H. Kratz, Modellbasierte Vorhersage der Zerspankräfte beim Schlichtfräsen von Freiformflächen, *wt-Werkstattstechnik*, 2001, **91**(5), p 280-284
7. L. Markworth, "Fünfschichtige Schlichtfräsbearbeitung von Strömungsflächen aus Nickelbasislegierungen," Dissertation, RWTH Aachen, 2005
8. M. Buschka, K. Weinert, and V. Petzoldt, Machining Properties of an Austenitic NiTi Shape Memory Alloy. Production Engineering—Research and Development, *Ann German Acad Soc Prod Eng*, 2002, **IX**(1), p 9-12
9. V. Petzoldt and K. Weinert, Deep Hole Drilling of NiTi Shape Memory Alloys, *Proceedings of the International Conference on Shape Memory and Superelastic Technologies SMST 2004*, October 3-7, Baden-Baden, M. Mertmann, Ed., 2006, p 259-264
10. V. Petzoldt and K. Weinert, Micromachining of NiTi Shape Memory Alloys. Production Engineering—Research and Development, *Ann. German Acad. Soc. Prod. Eng.*, 2006, **XIII**(2), p 43-46
11. D. Biermann, F. Kahleyß, and T. Surmann, Micromilling of NiTi Shape-Memory Alloys with Ball Nose Cutters, *Int. J. Mater. Manufact. Process.*, 2009, **24**(12), p 1266-1273
12. D. Biermann, K. Weinert, F. Kahleyß, and A. Baschin, Simultaneous 5-Axis Micro-Milling of NiTi Shape Memory Alloys, *Proceedings of the International Conference on Shape Memory and Superelastic Technologies*, 3-5 December 2007, Tsukuba, Japan, S. Miyazaki, Ed., ISBN 978-0-87170-722-2, p 447-454
13. K. Weinert and T. Surmann, Geometric Simulation of the Milling Process for Free Formed Surfaces. *Simulation Aided Offline Process Design and Optimization in Manufacturing Sculptured Surfaces*, January 2003, K. Weinert, Ed., p 21-30